Synthesis of controlled size starch nanoparticles (SNPs)

G. Gutiérrez[1], D. Morán[1], A. Marefati[2], J. Purhagen[2], M. Rayner[2], M. Matos[1,2*]

[1]Department of Chemical and Environmental Engineering, University of Oviedo, Julián Clavería 8, 33006 Oviedo, Spain

[2]Department of Food Technology, Engineering, and Nutrition, Lund University, P.O. Box 124, SE 22100 Lund, Sweden

*Corresponding author. Tel: +34 985 103029; Fax: +34 985 103434

E-mail address: matosmaria@uniovi.es

Abstract

Starch nanoparticles (SNPs) are a promising choice for the strategic development of new renewable and biodegradable nanomaterials for novel biomedical and pharmaceutical applications when loaded with antibiotics or with anticancer agents as target drug delivery systems. The final properties of the SNPs are strongly influenced by the synthesis method and conditions being a controlled and monodispersed size crucial for these applications.

The aim of this work was to synthesize controlled size SNPs through nanoprecipitation and microemulsion methods by modifying main operating parameters regarding the effect of amylose and amylopectin ratio in maize starches. SNPs were characterized by size and shape.

SNPs from 59 to 118 nm were obtained by the nanoprecipitation method, registering the higer values when surfactant was added to the aqueous phase. Microemulsion method led to 35-147 nm sizes observing a higher particle formation capacity. The composition of the maize used influenced the final particle size and shape.

Keywords

Starch nanoparticles, nanoprecipitation, microemulsion, size control, high amylose, waxy

Chemical compounds studied in this article

Sodium hydroxide (PubChem CID: 14798); Urea (PubChem CID: 1176); Absolute ethanol (PubChem CID: 702); CTAB (PubChem CID: 5974); Tween 20 (PubChem CID: 443314); Span 60 (PubChem CID: 3793749).

1. Introduction

Nanoparticles (NPs) are a promising choice for the strategic development of new drug delivery systems with novel applications in food, cosmetics and healthcare (Kim, Park, & Lim, 2015). Starch is a non-allergenic abundant polysaccharide in nature, renewable and biodegradable making it an ideal candidate as a component of green bio-formulations. The starch model is described as a concentric semi-crystalline multistate structure that can be involved in the production of new nano-elements. Starch nanoparticles are often referred to as starch nanocrystals. Some authors stated that the disruption of amorphous domains of semi-crystalline granules by acid hydrolysis will produce starch nanocrystals, while gelatinized starch will create SNPs (Le Corre, Bras, & Dufresne, 2010) that may include amorphous

matrices. However, other authors reported that it becomes almost impossible to clarify the terms starch nanocrystals and starch nanoparticles since both terms have been used to refer to the crystalline parts of starch remaining after hydrolysis or other physical treatments and suggest the general term SNPs is applied to describe the elements that have at least one dimension in the nanoscale (Kim et al. 2015).

The preparation of SNPs may be classified in two main different processes, bottom-up and top-down depending on the precursor material employed on the synthesis. In top-down processes, nanoparticles can be produced from structure and size refinement through a breakdown of larger voluminous materials or microparticles while in a bottom-up process, nanoparticles can be prepared from a buildup of atoms or molecules in a controlled manner in the form of small primary cores that is regulated by thermo-dynamic means such as self-assembly (Kim et al., 2015).

Another classification for top-down processes may be done according to the number of steps required to prepare the final SNPs involving simple or hybrid processes. Some of the most common top-down simple methods that have been known to produce SNPs are acid or enzymatic hydrolysis (Kim, Park, & Lim, 2008; Putaux, Molina-Boisseau, Momaur, & Dufresne, 2003). Hydrolysis involves long periods of time with low yields and resulting SNPs normally present more crystalline regions in starch granules since they are more resistant to the acid hydrolysis than the amorphous regions. LeCorre et al. investigated the influence of the botanic origin of starch on the final crystallinity of SNPs prepared using acid hydrolysis using an X-ray diffraction analysis. This study demonstrated that the most important parameter in determining the degree of crystallinity of SNPs was the amylose content in starch while no differences were observed when starches with different botanical origins but with similar amylose content were compared (LeCorre, Bras, & Dufresne, 2011).

On the other hand, physical treatments, such as high-pressure homogenization (Liua, Wua, Chen, & Chang, 2009), ultrasonication (Bel Haaj, Magnin, Pétrier, & Boufi, 2013) or extrusion (Son, Thio, & Deng, 2011) involve shorter periods of time with higher yields but it is difficult to control crystal destruction. Hybrid top-down processes have also been used with satisfactory results when a combination of both enzymatic and acid hydrolysis has been used for the preparation of SNPs since it was reported that the SNP preparation could be done within a reduced time by using the combined procedure (LeCorre, Vahanian, Dufresne, & Bras, 2012). There are also several studies in which hydrolysis was combined with a post-physical treatment of ultrasonication as final refinement (Kim, Han, Kweon, Park, & Lim, 2013; Kim, Park, Kim, & Lim, 2013b). However, ultrasonication may change the X-ray diffraction pattern of starch reducing crystallinity for longer periods of time.

Regarding bottom-up processes the most common methods of SNPs preparation are the microemulsion (Chin, Azman, & Pang, 2014; Chin, Nur, Yazid, & Pang, 2014b; Syahida, & Subash, 2016) and nanoprecipitation methods (Chin, Pang, & Tay, 2011; Chin, et al., 2014b; Ma, Jian, Chang, &Yu, 2008); Najafi, Baghale, & Ashori, 2016; Saari et al., 2017; Tan, Xu, Li, Liu, & Song, 2009). The nanoprecipitation process involves the successive addition of a dilute solution of polymer to a solvent which leads to the polymer nanoprecipitation based on its interfacial deposition following the

displacement of a semipolar solvent that is miscible with water. Microemulsion method involves the preparation of water-in-oil (W/O) microemulsions consisting of aqueous domains dispersed in a continuous oil phase stabilized by an interfacial film of surfactant molecules working as nanoreactors where the synthesis of the desired SNPs take place. This two approaches present many advantages since both are gentle chemical techniques with growing interest because large amounts of toxic solvents and external energy sources are avoided with efficient control of size, shape, monodispersity and composition of SNPs obtained (Chin et al., 2011; Chin et al., 2014a). Moreover, these preparation methods are the most common ones for encapsulation purposes.

The final properties of the SNPs are strongly influenced by the synthesis method and conditions, which in turn will determine its final applications. A controlled and monodispersed size is crucial for biomedical or pharmaceutical applications (Kumar et al., 2018). There have been indications of SNPs loaded with antibiotics (e.g., penicillin, ampicillin, ciprofloxacin, citoplastin) or biocide metals, such as Ag, having bacterial inhibition properties (Kumar et al., 2018; Likhitkar & Bajpai 2012; Najafi et al., 2016; Syahida, & Subash, 2016)) or with anticancer agents as target drug delivery systems (doxorubicin, docetaxel) (Dandekar et al., 2012; Xiao et al., 2006). However, some authors reported that the bactericidal properties were shown to be size-dependent and most effective in the 1-10 nm range (Kumar et al., 2018).

Therefore, this work aimed to synthesize controlled size SNPs with the use of bottom-up nanotechnology through nanoprecipitation and microemulsion methods by modifying main parameters involved, as injection rate, dissolution time, stirring rate, organic to aqueous phase ratio, as well as studying the effect of amylose and amylopectin ratio in maize starches. The SNPs were characterized by the size and shape using dynamic light Scattering (DLS) (Nanozetasizer from Malvern) and Scanning Electronic microscopy (SEM). X-Ray Powder Diffraction (XRPD) and Fourier transform infrared spectroscopy analysis (FTIR) were used to analyze the structure and crystallinity of both the granules and SNPs.

2. Materials and methods

2.1. Materials

Milli-Q water was used for all experiments to prepare the different aqueous phases while absolute ethanol was supplied by Sigma Aldrich (USA) as the main organic phase. Urea supplied by Serva Electrophoresis GmbH and NaOH provided by Panreac were used to formulate the different aqueous phases studied.

Maize starches with three different ratios of amylose and amylopectin, normal-, high amylose-, and waxy (high amylopectin) from Cerestar-AKV I/S (Denmark), were used in the study.

Cetyl Trimethyl Ammonium Bromide 99% (CTAB) was supplied by Sigma-Aldrich (USA). It is a quaternary ammonium salt, with a long alkyl group which present cationic surfactant properties with a hydrophilic-lipophilic balance (HLB) of 10. The hydrophilic-lipophilic balance (HLB) of an emulsifier is parameter that allows to classify surfactants for their lipophilic/hydrophilic character. This method is

based on the proportion between the weight percentages of the hydrophilic and lipophilic groups of a surfactant molecule (Griffin 1955).

CTAB was used to decrease the interfacial tension between water and ethanol during the nanoprecipitation process and study their effect on the resulting final SNPs size. The molecular formula is $C_{19}H_{42}BrN$ (MW=364.46 g/mol) and it has an appearance of white or almost white crystalline powder.

Two different non-ionic surfactants, Tween® 20 and Span® 60, were used to prepare SNPs by the microemulsion method, both were supplied by Sigma Aldrich (USA).

Tweens® or polysorbates are in simple terms ethoxylated chains. The solubility of Tweens® in aqueous solutions increases with the degree of ethoxylation. Tweens® are hydrophilic and are soluble or dispersible in water and dilute electrolytes solutions. Tween® 20 is a yellow viscous liquid, with a molecular formula of $C_{58}H_{114}O_{26}$ (MW=1227.54 g/mol) and its HLB of 16.7.

Sorbitan fatty acid esters are commercially known as Span®. All the Spans® have the structure of sorbitan (1,4-D-sorbitol anhydride) in common which is esterified with one or several fatty acids. Span® 60's HLB is 4.7 and has a molecular formula of $C_{24}H_{46}O_6$ (MW=430.62 g/mol).

Sunflower oil was purchased from the local supermarket, while soybean oil was supplied by Sigma Aldrich (USA). These two oils were used to formulate the microemulsions combined with Tween® 20 or Span® 60 as surfactants, ethanol as co-surfactant and Milli-Q water as the aqueous phase.

2.2. Methods

2.2.1. Nanoprecipitation method

Nanoprecipitation method was adapted from a method used in previus works by the nanoprecipitation of polymeric particles (Mathew & Dufresne, 2002). This process involves the successive addition of a dilute solution of dissolved starch to a solvent which leads to the starch precipitation.

First, 1% (w/v) starch solution was prepared by dissolving 0.2 g of starch into 20 mL of an aqueous phase by stirring at 80 °C for 30 or 60 min. Four different aqueous phase were tested: (i) 2 % (w/v) NaOH, (ii) 8 % (w/v) NaOH, (iii) 2 % (w/v) NaOH + 10% (w/v) urea, and (iv) 8 % (w/v) NaOH + 10 (%) (w/v) urea. Then, 1 mL of starch solution was added with a syringe pump (at injection rate: 2, 4 and 8 mL/h) into absolute ethanol (from 5 to 40 mL) under constant stirring (500 and 800 rpm).

The effect of the presence of surfactant in the aquoues phase was also studied. For these experiments 4 % (w/v) of CTAB was added to the aqueous phase.

2.2.2. Microemulsion method

Microemulson method was based on the addition of an aqueous starch solution to an organic solvent including a surfactant while being homogenized to form a fine water-in-oil microemulsion where nanoparticles precipitate (Qiu et al., 2020).

First, 1 % (w/v) starch solution was prepared by dissolving 0.2 g of starch into 20 mL of an aqueous phase by stirring at 80 °C for 30 min. Then, 1 mL of starch solution prepared was added with a syringe pump at 4 mL/h into the organic phase (30 mL) under constant stirring (500 rpm).

The organic phase was formed by ethanol with 1 % (w/v) of oil (soybean or sunflower) and two different

surfactants used as stabilizers: Tween® 20 and Span® 60 at three different concentrations being 0.1, 1 and 3% (w/v). To prepare the organic phase the surfactant and the oil were added to absolute ethanol and gently mixed for an hour. The presence of ethanol will act as co-stabilizers enhancing the spontaneous microemulsion formation (Syahida & Subash, 2016; Najafi et al., 2016; Chin et al., 2011).

2.3. SNPs characterization

2.3.1. Particle size distribution

Size (in number) and homogeneity (PdI) of particles were measured by Dynamic Light Scattering (DLS) using a Zetasizer Nano ZS equipment (Malvern Instruments Ltd, Malvern, UK). First, the samples were centrifuged at room temperature at 1000 rpm for 10 min. The supernatant was removed to obtain the SNPs in the form of pellets which were washed twice to remove the remains of NaOH and urea, primarily with absolute ethanol and then with Milli-Q water centrifuging again at the same conditions between each wash. Samples were measured with the 173° backscatter detector in disposable low volume cuvettes (Malvern Instruments Ltd, Malvern, UK).

2.3.2. Morphology and size

The shape and size of SNPs were analyzed using a JEOL JSM-6610 LV field emission Scanning Electron Microscope at an acceleration voltage of 20 kV. Samples were washed in ethanol and then dehydrated in a heater for 24 h at 80 °C. Dehydrated samples were fractured with a spatula and fragments were mounted on aluminum SEM stubs and coated with gold in Balzers SCD 004 sputter coater (Bal-Tec AG, Liechtenstein) before the analysis. The average particle size of the SNPs was determined by random measurements using ImageJ software.

2.3.3. X-Ray Powder Diffraction (XRPD) analysis

The crystalline structure of the starch granules and the synthesized SNPs have been determined by X-Ray Powder Diffraction (XRPD) analysis. The X-ray powder diffraction data for the samples were collected, at RT, using $CuK_{\alpha 1,2}$ radiation (λ= 1.54056 Å and 1.54439 Å) in a Bragg-Brentano reflection configuration, on PHILIPS X' PERT PRO Panalytical diffractometer in a 2θ range of 5–27°, with a step size of 0,08356.

2.3.4. Fourier transform infrared spectroscopy analysis (FTIR)

FTIR spectra were acquired in a Fourier Transform Infrared Spectrophotometer (Varian 620-IR, Thermo Fisher ScientificInc., U.S.A.) at room temperature. Samples, dried powder and approximately 1 mg, were directly measured, and spectra were recorded between 650 - 4000 cm−1 (medium infrared band).

3. Results and discussion

3.1. Nanoprecipitation method

3.1.1. Screening of operating conditions

To do an initial screening of operating variables affecting the process, the injection rate was varied (2, 4 and 8 mL/h), the dissolution time (30 and 60 min) and stirring rate (500 and 800 rpm). Results are shown in Table 1 and Figure 1.

It was observed that the mean particle sizes decreased as the injection rate increased. However, it seemed

that higher particle formation capacity and more spherical SNPs were obtained when the medium injection rate, i.e., 4 mL/h, was used (Sample N2 from Fig 1) . Regarding the effect of the stirring rate, although no large differences were found on mean sizes, it was observed that SNPs were laminar in shape instead of spherical at the highest stirring rate (Sample N4 from Fig 1). In addition, the results showed that by increasing the aqueous phase dissolution time, a larger amount of agglomerates were produced (Sample N5 from Fig 1).

Taking these results into account, the operating conditions selected were 4 mL/h of injection rate, 30 minutes of aqueous phase dissolution time and 500 rpm of stirring rate.

3.1.2. Effect of aqueous phase formulation

Different formulations for the aqueous phase used to nanoprecipitate the SNPs were in terms of NaOH and urea solutions since it was reported in previous studies performed with cellulose and starch that the presence of NaOH breaks the intermolecular interactions and intramolecular hydrogen bonds of starch molecules, while urea plays an important role in preventing the self-association of starch molecules, which leads to greater solubility of starch powder (Chin et al., 2011; Jin, Zha, & Gu, 2007).

To determine the best aqueous phase formulation, experiments were carried out with each one of them using the nanoprecipitation method with an initial volume of ethanol of 20 mL as an organic phase, a constant stirring speed during the injection of 500 rpm and a pumping flow rate of 4 mL/h. These parameters were determined based on the literature as well as some preliminary experiments (Chin et al., 2011, Chin et al., 2014). Subsequently, the particle size and PdI were characterized by DLS and results are shown in Table 1. SNPs were also observed under SEM (Figure 1) and the size was measured using ImageJ. In addition, shape was also observed since the shape of SNPs depends on synthesis conditions, they can be rod-like in shape, spherical or a mixture of both (Chien et al., 2011).

It was observed that SNPs were obtained with all of the aqueous phases tested. However, non-spherical shape for SNPs was obtained when 2% (w/v) NaOH solution was used (Sample N6 from Fig 1). The number of nanoparticles obtained was greater for urea-containing formulations, as expected. In fact, for the 8% (w/v) NaOH and 10% urea (w/v) solution, fewer agglomerates were observed obtaining an average particle size around 75.1 nm, measured on the micrographs (Sample N2 from Fig 1). Therefore, this formulation was selected for subsequent experiments. Size obtained with DLS was around 30 nm in number with a PdI of 0.43. This discrepance can be explained by the fact that particle size varied in a fairly wide range (25 nm to 100 nm), which is in good agreement with the PdI obtained, but it was observed that small particles were predominated, which is consistent with the data obtained in number by the DLS technique.

3.1.3. Effect of ratio of organic phase versus aqueous phase

The effect of different ratios of organic: aqueous phase on the formulation of SNPs was studied since in previous studies it was observed that this ratio could affect the final shape of the SNPs (Chin et al., 2011). The ratios tested were: 5:1, 10:1; 15:1, 20:1, 25:1, 30:1 and 40:1 using in all the experiments ethanol as the organic phase. Results are shown in Table 1 and SEM micrographs are shown in Figure

1. Spherical SNPs were observed at a ratio interval of 20:1-30:1 (Samples N2, N12 and N13 from Fig 1). At lower ratios, fibrous shaped SNPs were obtained while mixtures of fibers and spheres were obtained when higher ratios were used (Sample N14 from Fig 1). These results were in good agreement with previously reported by Chin et al. (2011).

226 *Table 1. Mean sizes and PdI of SNPs obtained by the nanoprecipitation method using normal maize starch at different operating conditions and formulations*

Sample	Type of starch	Aqueous phase (% w/v)	Flow rate (mL/h)	Stirring (rpm)	Dissolution time (min)	O:A ratio (mL/mL)	Size (nm) Number	PdI	ImageJ (nm)
N1	Normal	NaOH 8% + urea 10%	2	500	30	20:1	42.6±27.5	0.44±0.01	---[1]
N2	Normal	NaOH 8% + urea 10%	4	500	30	20:1	29.7±77.4	0.43±0.04	75.1±39.8
N3	Normal	NaOH 8% + urea 10%	8	500	30	20:1	13.9±9.03	0.46±0.01	67.2±19.9
N4	Normal	NaOH 8% + urea 10%	4	800	30	20:1	25.1±10.5	0.34±0.04	---[1]
N5	Normal	NaOH 8% + urea 10%	4	500	60	20:1	23.2±8.62	0.61±0.01	77.6±23.3
N6	Normal	NaOH 2%	4	500	30	20:1	42.8±43.1	0.32±0.06	---[1]
N7	Normal	NaOH 8%	4	500	30	20:1	15.8±4.34	0.39±0.07	66.1±12.6
N8	Normal	NaOH 2% + urea 10%	4	500	30	20:1	55.2±32.2	0.23±0.02	74.6±17.3
N9	Normal	NaOH 8% + urea 10%	4	500	30	5:1	316±56.8	0.59±0.03	---[1]
N10	Normal	NaOH 8% + urea 10%	4	500	30	10:1	34.9±9.59	0.66±0.03	---[1]
N11	Normal	NaOH 8% + urea 10%	4	500	30	15:1	34.3±10.3	0.79±0.16	---[1]
N12	Normal	NaOH 8% + urea 10%	4	500	30	25:1	23.3±6.23	0.46±0.04	63.3±33.8
N13	Normal	NaOH 8% + urea 10%	4	500	30	30:1	24.5±4.53	0.47±0.08	59.1±28.5
N14	Normal	NaOH 8% + urea 10%	4	500	30	40:1	24.4±5.77	0.39±0.08	---[1]
N15	Waxy	NaOH 8% + urea 10%	4	500	30	20:1	22.3±24.4	0.37±0.05	63.1±22.6
N16	Waxy	NaOH 8% + urea 10%	4	500	30	30:1	26.2±3.83	0.43±0.03	58.8±15.6
N17	High amylose	NaOH 8% + urea 10%	4	500	30	20:1	29.3±16.7	0.44±0.03	73.6±20.5
N18	High amylose	NaOH 8% + urea 10%	4	500	30	30:1	16.4±6.70	0.48±0.01	72.6±12.2
N19	Normal	NaOH 8% + urea 10% + 4%CTAB	4	500	30	20:1	126±40.8	0.47±0.12	---[1]
N20	Normal	NaOH 8% + urea 10% + 4%CTAB	4	500	30	30:1	56.7±8.95	0.42±0.04	---[1]
N21	Waxy	NaOH 8% + urea 10% + 4%CTAB	4	500	30	20:1	50.3±8.63	0.61±0.12	---[1]
N22	Waxy	NaOH 8% + urea 10% + 4%CTAB	4	500	30	30:1	36.6±8.15	0.45±0.05	117±47.1
N23	High amylose	NaOH 8% + urea 10% + 4%CTAB	4	500	30	20:1	> 500	0.63±0.10	65.6±21.3
N24	High amylose	NaOH 8% + urea 10% + 4%CTAB	4	500	30	30:1	> 300	0.53±0.03	64.3±13.8

227 [1] Non spherical SNPs

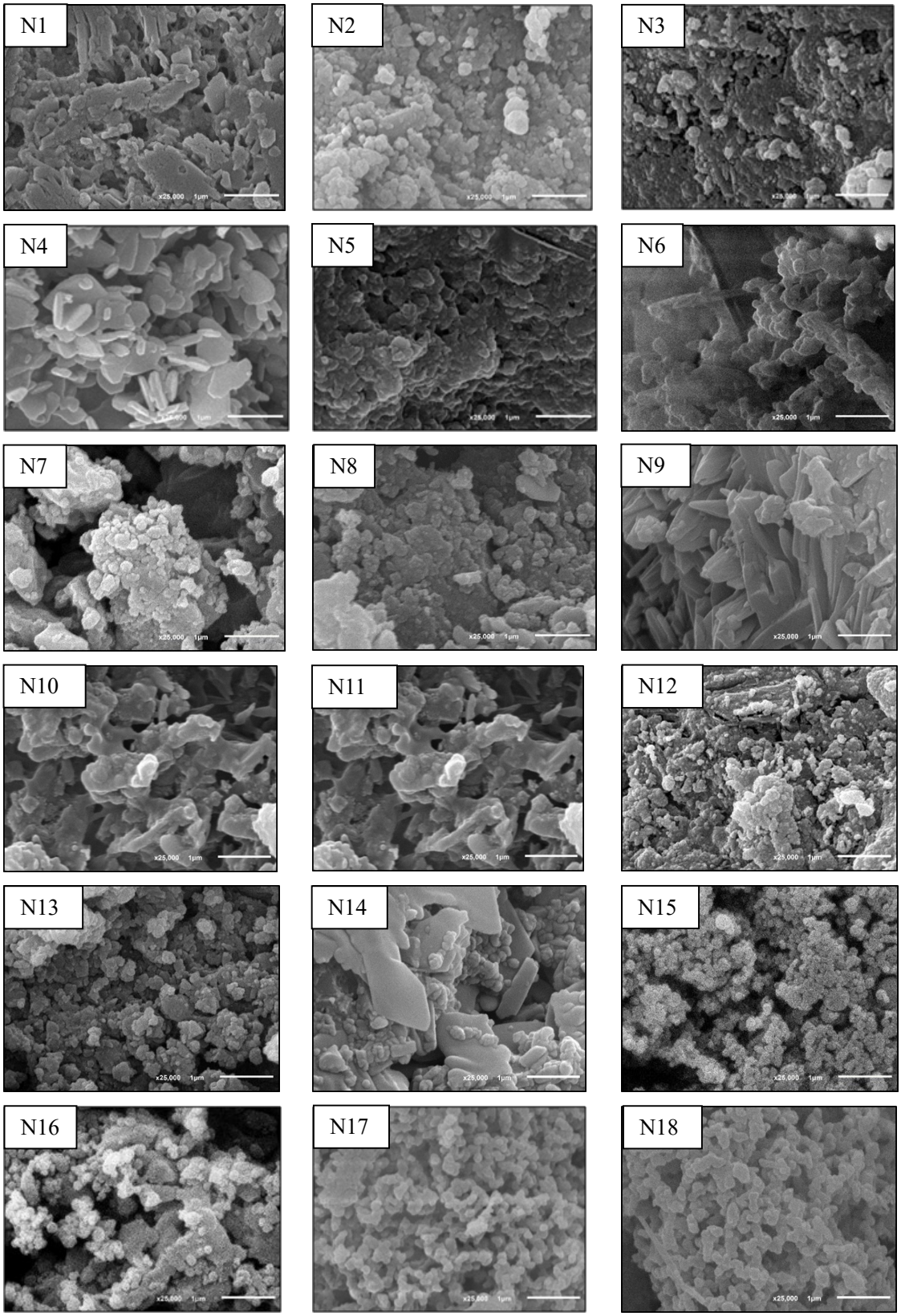

228 *Figure 1. SEM micrographs of SNPs obtained by the nanoprecipitation method using different operating*
229 *conditions and different formulations by nanoprecipitation method*
230

3.1.4. Effect of amylose/amylopectin content

Three maize starches were used to investigate the effect of amylose/amylopectin content on the SNPs size formation. The results are presented in Table 1 and Figure 1. Samples N2 and N13 are refered to normal maize starch, samples N15 and N16 to waxy maize starch and samples N17 and N18 to high amylose maize starch. Smaller particle sizes were obtained when the waxy starch was used, obtaining an average size measured with ImageJ of 63.1 nm and with a 20:1 ratio organic: aqueous phase. When the ratio was 30:1 an average size of 58.8 nm was obtained. While when the starch with high amylose content was used, SNPs average size was 73.6 nm for a 20:1 ratio and 72.6 nm when a 30:1 ratio was used.

By looking at the pictures, normal maize seemed to give two different distributions of particle sizes. For waxy starch, the particles seem to be smaller and tender to cluster, while for high amylose, the particles seem to be more rod-like and forming kind of a pearl string. When comparing this to the molecular structure of the different starches, normal starch contains both amylose and amylopectin which means the presence of two different sized molecules with different structures, waxy is highly branched molecule and amylose is a long chain molecule with just a few branches. Therefore, how the SNPs are organized in these images seems to be correlated with the structure of the pure starch molecules of the intact granules when comparing them.

3.1.5. Effect of surfactant addition

The effect of surfactant addition on the mean particle sizes of SNPs formed was studied since surfactants can interfere with the interfacial tension between the organic and the aqueous phase during the nanoprecipitation process. For this purpose, the best organic: aqueous phase ratios were used (20:1 and 30:1) to synthesize SNPs using CTAB for the three types of starches studied as it was demonstrated in previous studies that led to smaller sizes (Chin et al., 2011). The main results obtained are shown in Table 1 and Figure 2 (samples from N19 to N24).

No differences in shape were observed when normal maize starch was used in presence of CTAB (Figure 2, samples N19 and N20). However, SNPs obtained with waxy starch in the presence of CTAB led to a mixture of spherical particles and rod-shaped particles (Figure 2, samples N21 and N22) while for starch with high amylose content, spherical particles predominated (Figue 2, samples N23 and N24). In general, when comparing sizes in number for the three types of starches they were smaller without the presence of surfactant (Table 1). Moreover, non spherical particles were observed under SEM for waxy and normal starches. However for high amylose SNPs size was reduced around 8-9 nm probably caused by the interactions between high amylose starch molecules and CTAB surfactant that could improve starch SNPs stability by reducing particle agglomeration. It has been demonstrated in previous studies that interactions between amylose and amylopectin with CTAB seemed to be similar but with small differences probably caused by the different structure (Lundqvist, Eliaason, & Olofsson, 2002a, 2002b).

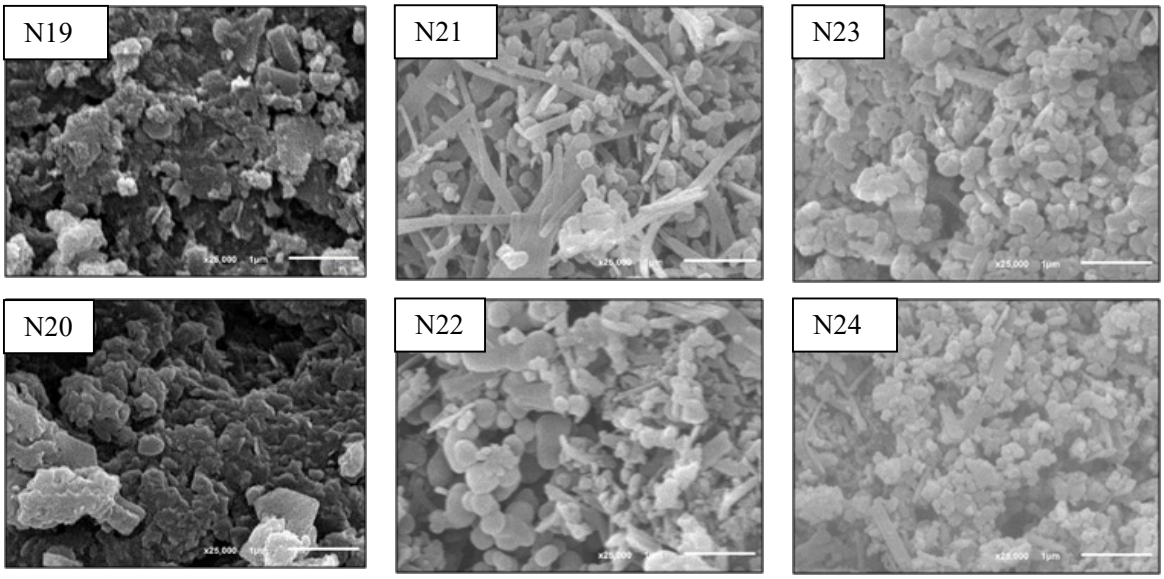

Figure 2. SEM micrographs of SNPs obtained by the nanoprecipitation method using an aqueous phase consisting of 8% (w/v) NaOH and 10% (w/v) solution and 4 % (w/v) of CTAB using starches with different amylose/amylopectin content and different organic:aqueous phase ratios

3.2. Microemulsion method

3.2.1. Effect of microemulsion formulation

The results obtained are shown in Table 2 and Figure 3.

Table 2. Mean sizes and PdI of SNPs obtained by ME method using an aqueous phase consisting of 8 % (w/v) NaOH and 10 % (w/v) solution with normal starch and different type of oil (1 % w/v) and surfactants as well as different concentrations of surfactant

Sample	Type of starch	Oil	Surfactant (% w/v)	Size (nm) Number	PdI	ImageJ (nm)
M1	Normal	Soybean oil	0.1%T20	62.3±11.4	0.55±0.03	59.9±14.4
M2	Normal	Sunflower oil	0.1%T20	41.8±3.85	0.56±0.07	59.6±16.2
M3	Normal	Soybean oil	0.1%S60	66.3±26.7	0.52±0.04	81.2±15.1
M4	Normal	Sunflower oil	0.1%S60	46.8±5.33	0.54±0.03	63.9±17.5
M5	Normal	Soybean oil	1% T20	31.0±59.9	0.74±0.04	46.4±14.9
M6	Normal	Sunflower oil	1 % T20	58.1±12.8	0.72±0.05	61.7±14.7
M7	Normal	Soybean oil	1% S60	60.4±14.7	0.67±0.09	64.6±15.1
M8	Normal	Sunflower oil	1% S60	51.5±13.8	0.69±0.11	49.6±9.25
M9	Normal	Soybean oil	3% T20	56.5±13.8	0.53±0.09	43.8±11.8
M10	Normal	Sunflower oil	3% T20	53.4±17.3	0.54±0.01	52.9±11.5
M11	Normal	Soybean oil	3% S60	112±50.3	0.39±0.04	120±44.5
M12	Normal	Sunflower oil	3% S60	61.1±38.8	0.37±0.04	---[1]

[1] Non spherical SNPs

For 1% (w/v) oil spherical particles were obtained in all cases with the same average particle size of 60 nm (sample M1) measured with ImageJ, for the formulations containing 0.1% (w/v) Tween 20 and either

soybean or sunflower oil. On the other hand, formulations with 0.1% (w/v) Span 60 gave rise to larger SNPs for both oils tested. This differences in size could be attributed to the different hydrophilicty of the different types of the surfactants used what could modify the interactions between starch particles. Tween 20 is more hydrophilic than Span 60, and would interact stronger with starch molecules, and therefore smaller SNPs could be precipitated. A similar trend was observed by other authors when two surfactants with different HLB were tested (Chin et al., 2011).

Increasing the amount of surfactant to a 1% (w/v), a decrease of around 10-20 nm was observed in the SNP sizes for both surfactants and oil used.. This could be explained by the fact that at higher surfactant concentrations microemulsions with smaller droplet size could be obtained producing at the same time a decrease in the resulting SNPs formed. Following formulations used by other authors, it was observed that 3% seemed to be enough to stabilize the interface during SNPs formation and controlling the size (Chin et al., 2014).

On the other hand, a different trend was found when Span 60 was used since a large increase in the average particle size was observed, with values up to 120 nm (sample M11), when soybean oil was used while particles that did not present spherical form, as shown in Figure 3 (sample M12), were obtained with the formulation with sunflower oil.

It can be observed that, compared to results obtained by the nanoprecipitation method, particle formation capacity obtained by microemulsion method seemed to be higher in all cases.

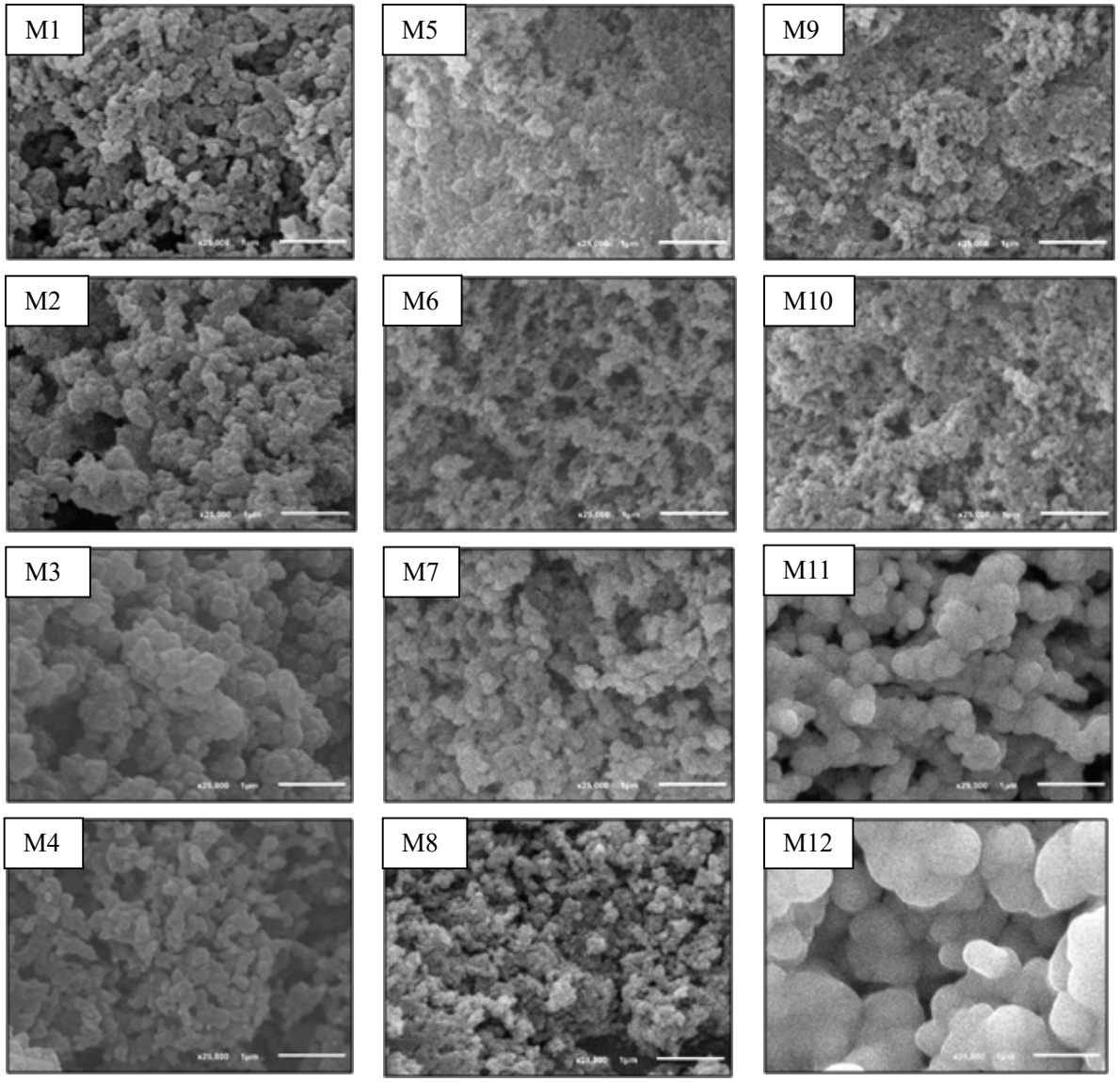

Figure 3. *SEM micrographs of SNPs obtained by ME method using an aqueous phase consisting of 8 % (w/v) NaOH and 10 % (w/v) solution and different type of oil (1 %) and surfactants (0.1, 1 or 3 % w/v)*

3.2.2. Effect of amylose and amylopectin content

All results are shown in Table 3, Figure 4 and Figure 5. Sizes obtained with waxy and high amylose starches with microemulsion method presented higher dependence to the microeoemulsion formulation than the ones obtained with normal starch, being high amylose starch the one that present more variations on the SNPs size registered in all formulations tested.

Table 3. *Mean sizes and PdI of SNPs obtained by ME method using an aqueous phase consisting of 8 % (w/v) NaOH and 10 % (w/v) solution with waxy and high amylose starch and different concentrations of surfactant at 1 % (w/v) sunflower/soybean oil content and 30:1 ratio of organic to aqueous phase*

Sample	Type of starch	Oil	Surfactant (%w/v)	Size (nm) Number	PdI	ImageJ (nm)
M13	Waxy	Soybean oil	0.1% T20	22.9±9.21	0.43±0.01	38.9±11.7
M14	Waxy	Sunflower oil	0.1% T20	24.6±10.1	0.40±0.01	---[1]
M15	Waxy	Soybean oil	0.1% S60	38.5±20.9	0.37±0.03	84.3±16.4
M16	Waxy	Sunflower oil	0.1% S60	48.7±63.7	0.24±0.01	78.4±14.8
M17	Waxy	Soybean oil	1% T20	38.8±20.8	0.36±0.05	---[1]
M18	Waxy	Sunflower oil	1% T20	30.9±15.5	0.38±0.04	---[1]
M19	Waxy	Soybean oil	1% S60	44.9±13.1	0.61±0.10	84.8±23.4
M20	Waxy	Sunflower oil	1% S60	52.8±15.1	0.49±0.08	62.6±28.3
M21	Waxy	Soybean oil	3% T20	36.9±17.9	0.27±0.01	46.5±12.7
M22	Waxy	Sunflower oil	3% T20	38.1±14.1	0.33±0.01	---[1]
M23	Waxy	Soybean oil	3% S60	81.5±24.3	0.62±0.11	---[1]
M24	Waxy	Sunflower oil	3% S60	59.2±24.1	0.39±0.04	---[1]
M25	High amylose	Soybean oil	0.1% T20	61.7±8.80	0.69±0.16	75.4±17.8
M26	High amylose	Sunflower oil	0.1% T20	90.8±23.4	0.99±0.01	106±26.5
M27	High amylose	Soybean oil	0.1% S60	65.3±8.29	0.79±0.27	54.5±13.2
M28	High amylose	Sunflower oil	0.1% S60	82.5±35.3	0.62±0.08	114±49.7
M29	High amylose	Soybean oil	1% T20	67.2±28.6	0.58±0.05	55.4±11.1
M30	High amylose	Sunflower oil	1% T20	73.6±10.6	0.80±0.09	40.9±10.5
M31	High amylose	Soybean oil	1% S60	78.3±10.9	0.89±0.14	134±32.2
M32	High amylose	Sunflower oil	1% S60	72.1±34.5	0.65±0.16	147±28.8
M33	High amylose	Soybean oil	3% T20	107±26.3	0.49±0.05	34.8±10.1
M34	High amylose	Sunflower oil	3% T20	54.2±57.3	0.46±0.08	---[1]
M35	High amylose	Soybean oil	3% S60	113±67.2	0.26±0.01	129±28.2
M36	High amylose	Sunflower oil	3% S60	77.9±41.9	0.68±0.12	---[1]

[1] Non spherical SNPs

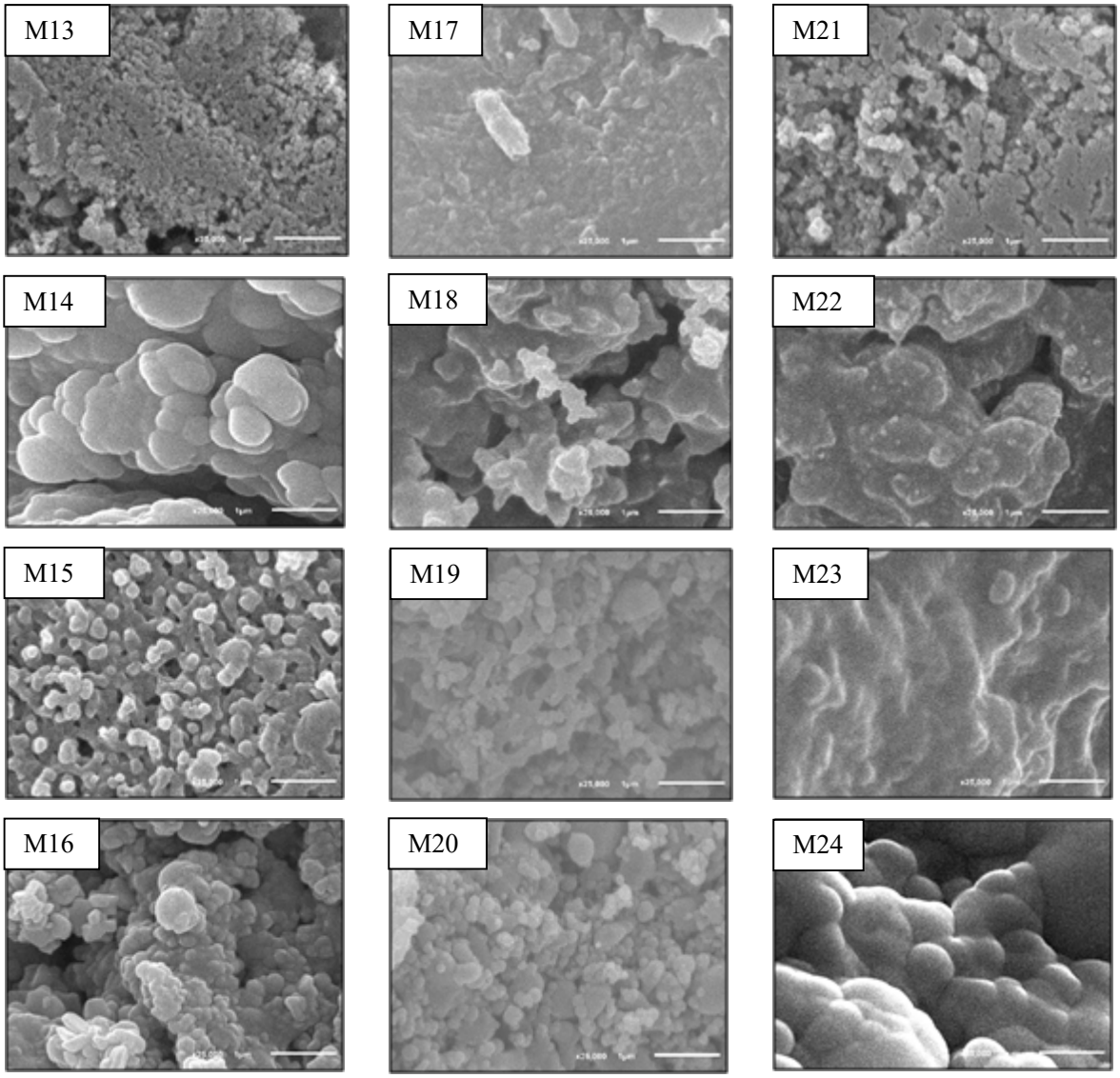

Figure 4. SEM micrographs of waxy SNPs obtained by ME method using an aqueous phase consisting of 8% (w/v) NaOH and 10% (w/v) solution, waxy starch and different type of oil (1%) and surfactants (0.1, 1 or 3%)

Best results were obtained at lower surfactant concentrations. Comparing both types of starch used smaller average size, 38.9 nm, measured with ImageJ, was obtained when 0.1% (w/v) surfactant of Tween 20 was used for waxy starch when using soybean oil (sample M13) while a mean size of 75.4 nm was obtained for high amylose starch (sample M25). The opposite trend was found with Span 60 when the same oil was used since the sizes obtained were 84.3 nm and 54.5 nm when waxy (sample M15) and high amylose (sample M27) starches were used respectively.

Using sunflower oil, the average size was 106 nm when 0.1% (w/v) Tween 20 was used with high amylose starch (sample M26) while non spherical particles were obtainedwhen usign waxy starch. When the surfactant was used with Span 60 at the same concentration the average sizes was 78.4 nm for the waxy starch (sample M16) and 114 nm using high amylose starch (sample M28). Furthermore, when the amount of the surfactant was increased to 1% (w/v), particles were not formed for Tween 20 and

waxy starch with both types of oil. However, using 1% (w/v) Span 60 the average size obtained was 84.8 nm (sample M19) and 62.6 nm (sample M20) when soybean and sunflower oil were used respectively.

When high amylose starch was used, a smaller average size was obtained (55.4 nm) (sample M29) with soybean oil and 1% (w/v) Tween 20 and 134 nm (sample M31) for 1% (w/v) Span 60. A similar trend was found when sunflower oil was used with the same type of starch with the average size of 40.9 nm (M30) for 1% (w/v) Tween 20 while particles with a size of 147 nm (sample M32) were obtained with the Span 60. This is an indications that Span 60 presents a negative effect on high amylose SNPs formation as was the case for normal starch.

At soybean oil and 3% (w/v) Tween 20 concentration, an average size of 34.8 nm was obtained for high amylose starch (sample M33) and 46.5 nm with waxy starch (sample M21).

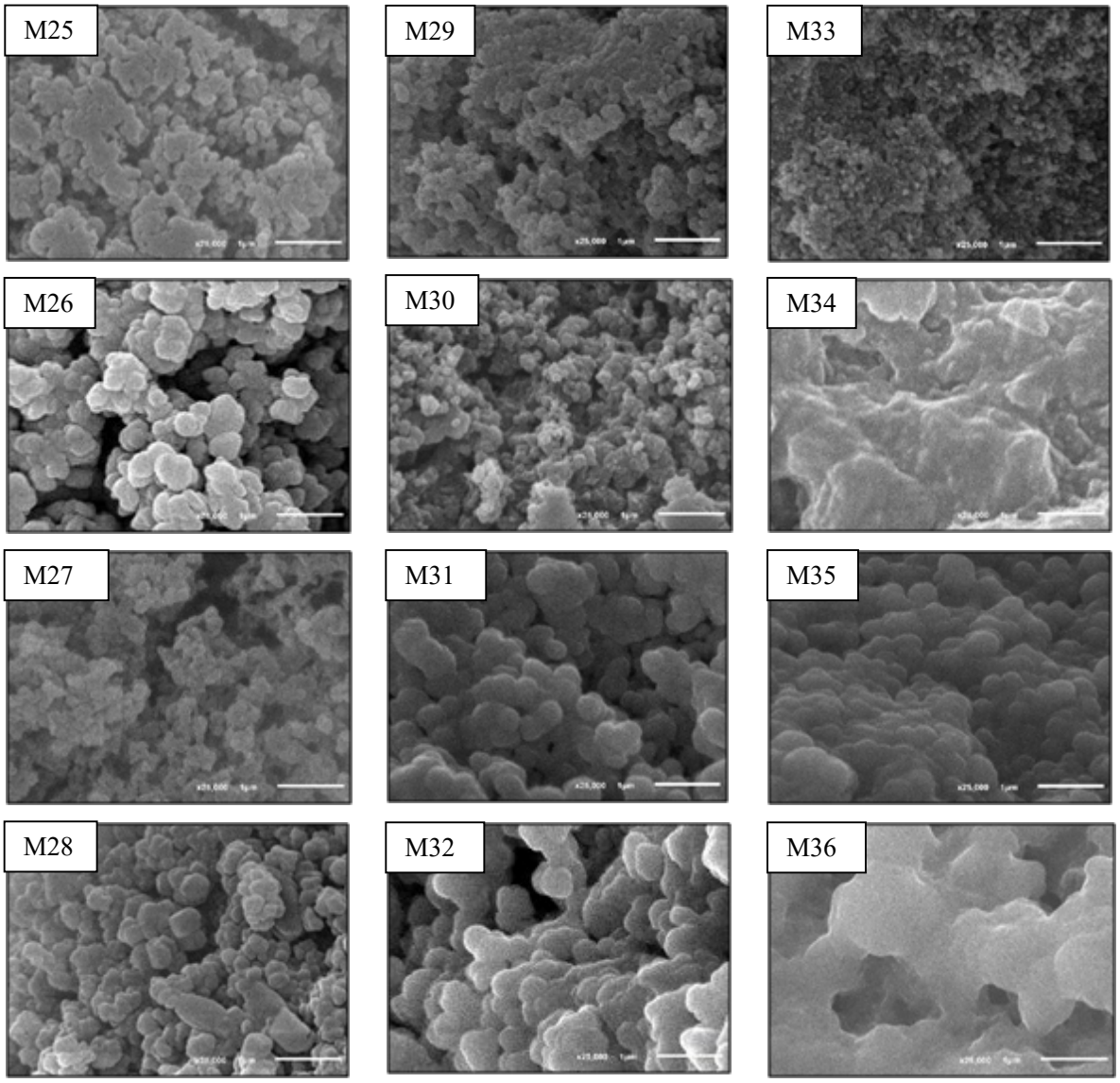

Figure 5. SEM micrographs of high amylose SNPs obtained by ME method using an aqueous phase consisting of 8 % (w/v) NaOH and 10 % (w/v) solution, waxy starch and different type of oil (1 %) and surfactants (0.1, 1 or 3 % w/v)

Results obtained with the rest of the formulations containing 3% (w/v) Span 60 did not show spherical shape but aggregates which means that SNPs were not formed completely what could be caused because of using a high volume of a hydrophobic surfactant, probably caused by interactions between the hydrocarbon chains.

3.3. XRPD and FTIR analysis

The three types of granules used in this study were analysed by FTIR as well as the resulting SNPs prepared with each type of granules by the two methods of preparation used (nanoprecipitation and microemulsion), using the operational conditions that led best results, being in total 9 samples analysed. The FTIR spectra depicted in Figure 6 shows almost identical characteristic bands for the three types of starch granules studied. The strong absorption peak was observed around 3280–3243 cm^{-1} which is attributed to is attributed to overlapping of stretching bands of the different -OH groups. Similar results were obtained by other authors (Ahmad et al., 2020; Acevedo-Guevara et al., 2018).

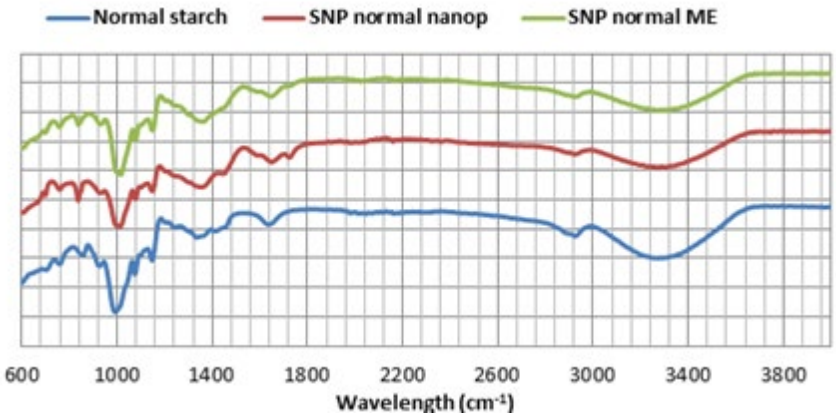

(A) Normal starch granules, nanoparticles: N2 and M1

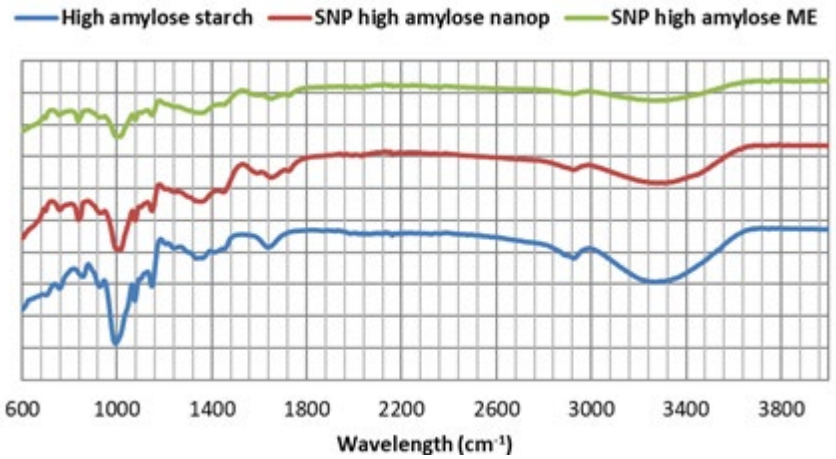

(B) High amylose starch granules, nanoparticles: N17 and M30

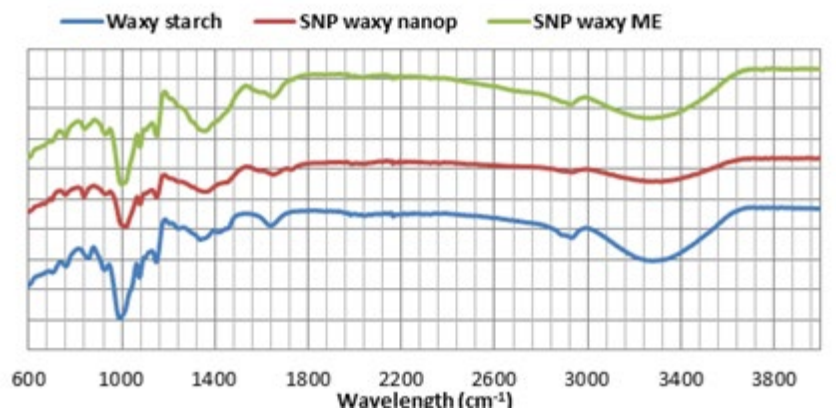

(C) Waxy starch granules and nanoparticles: N15 and M20

Figure 6. FTIR curves of normal, waxy and high amylose starches and the resulting SNPs synthesized at optimum conditions. ME: Microemulsion method; nanop: Nanoprecipitation method

However, Ahmad *et al*. also reported that the peaks of O–H stretching shifted to higher wavelength range for SNPs, obtained by alkalization and sonication processes, what was attributed to the loss of the crystalline structure and exposure of -OH groups of the starch molecule to the preparation process (Ahmad *et al*. 2020). Moreover, in the FTIR images obtained in that study it can be observed how the intensity of the absorption peaks within that wavelength is much less pronounced for the SNPs. A similar

trend was observed for SNPs obtained by nanoprecipitation and ME methods for the three types of starches.

The absorption peak observed at 2927 cm^{-1} can be explained by -CH_2 stretching vibrational modes bands while the peaks observed at the wavelengths of 1147, 1078 and 990 cm^{-1} are associated with the stretching vibration of the C-O bond, C-O-H and C-O-C groups in the glucose ring, respectively. The absorption peak at 1643 cm^{-1} can be due to the presence of bound water in starch. This is in good agreement with prvious studies (Ahmad t al, 2020; Qiu t al., 2016).

FTIR spectroscopy can also be used to determine the crystallinity of starch by characterizing the changes that occur in the semi crystalline and amorphous domains within starch granules (Ahmad *et al*., 2020). The high peak intensity obtained at 995 cm^{-1} that possess shoulder at the wavenumber of 1018 cm^{-1} and 1047 cm^{-1} indicated amorphous character and crystalline order of starch. No differences were observed when comparing the spectra within this range for normal maize starch granules and SNPs produced by both methods of preparation. However, for high amylose starch a less pronounced peak was observed when SNPs were obtained by the ME method. Similar trend was found when comparing the spectra obtained with waxy starch regarding a different absorption with SNPs obtained by nanoprecipitation. Therefore, the type of starch used and the method of preparation selected for the synthesis of SNPs could produce some changes in the physico-chemical structure of the resulting nanoparticles.

The same samples were analysed by XRPD in order to observe the crystalline structure of the granules and the spectra are shown in Figure 7.

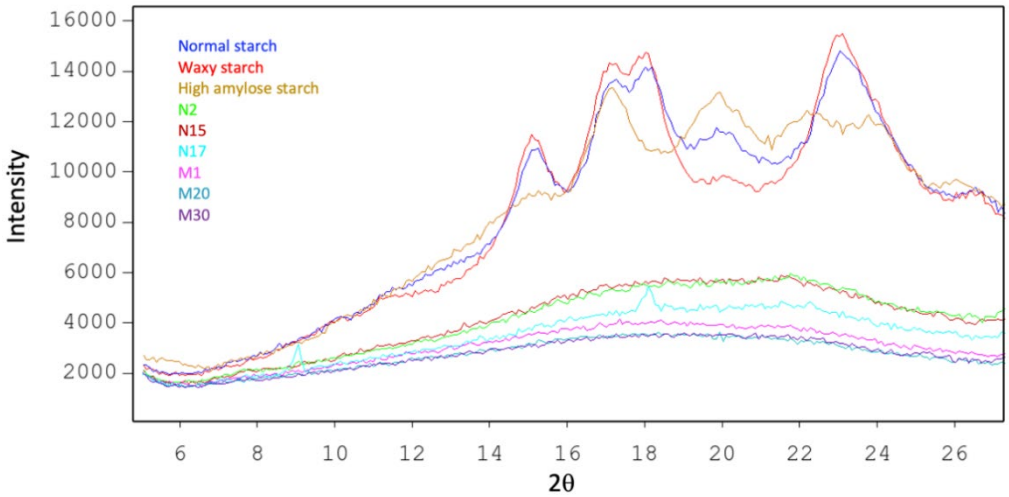

Figure 7. XRPD spectra of normal, waxy and high amylose starches and the resulting SNPs synthesized at optimum conditions. ME: Microemulsion method (samples M1, M20 and M30); nanop: Nanoprecipitation method (samples N2, N15 and N17)

The A-type X-ray diffractions patterns were observed for normal and waxy maize starch granules with peaks at Bragg angles (2θ) at 15°, 17°, 18° and 23°. High amylose starch exhibited B+V type crystalline

pattern displaying the peaks at 17.1°, 19.9°, 22.3° and 24.9°. These results are in good agreement with previous studies (Lin et al., 2020.).

On the other hand, major peak diffraction did not exist for all SNPs analysed appearing the whole structure like amorphous. Similar results were reported by other authors (Ding et al., 2018). Moreover, it was also reported that low X-ray crystallinity is not necessary related to poorly ordered starch molecules, but may be the result of small size crystallite in the granules (Kibar et al., 2010). Therefore, the small size of the SNPs reported in the manuscript could explain the XRD spectra obtained.

4. Conclusions

Nanoprecipitation method allowed to produce maize SNPs in the range 58-73 nm, at optimum conditions, while by the use of microemulsion method sizes between 35-147 nm were registered, obtaining the smaller sizes when waxy maize starch was used in both techniques. The type of oil used for microemulsion formulation did not present a high influence on the SNPs size but the type of surfactant was a key factor, as a general trend smaller sizes were obtained by the use of very hidrophilic surfactants. Comparing both methods of preparation, higher particle formation capacity was observed by microemulsion method with a more monodispersed and discrete appearance without the presence of large agglomerates. Therefore, controlled size SNPs could be obtained by this microemulsion method selecting the appropiate formulation and starch type.

Acknowledgements

This work was supported by Ministerio de Economía y Empresa (MINECO, Spain) under Grant MAT2017-84959-C2-1-R. This study was also cofinanced by Consejería de Educación y Ciencia del Principado de Asturias (Ref. IDI/2018/000185). A travel Grant from Lunds Tekniska Högskola (LTH) and from Ersasmus + from University of Oviedo (Ref. STT1819) was also received to perform a research stay at Department of Food Technology, Engineering and Nutrition (Lund University).

5. References

Acevedo-Guevara, L., Nieto-Suaza, L., T. Sanchez, L.,Pinzon, M.I., Villa, C.C.. (2018)Development of native and modified banana starch nanoparticles as vehicles for curcumin *International Journal of Biological Macromolecules* 111, 498–504.

Ahmad, M., Gani, A., Hassan, I., Huang, Q., Shabbir,H. (2020) Production and characterization of starch nanoparticles by mild alkali hydrolysis and ultra-sonication process. *Scientific Reports* 10:3533 https://doi.org/10.1038/s41598-020-60380-0.

Chin, S.F., Azman, A., & Pang, S.C. (2014). Size Controlled Synthesis of Starch Nanoparticles by a Microemulsion Method. *Journal of Nanomaterials, ID763736*. doi.org/10.1155/2014/763736.

Chin, S.F., Nur, S., Yazid, A.M., Pang, S.C. (2014b). Preparation and Characterization of Starch Nanoparticles for Controlled Release of Curcumin, *International Journal of Polymer Science, ID340121*. doi.org/10.1155/2014/340121.

Chin, S.F., Pang, S.C., & Tay, S.H. (2011). Size controlled synthesis of starch nanoparticles by a simple nanoprecipitation Method. *Carbohydrate Polymers,* 86, 1817– 1819.

Dagang L, Qinglin W., Huihuang C., Peter R. C. (2009). Transitional properties of starch colloid with particle size reduction from microto nanometer. *Journal of Colloid and Interface Science, 339*, 117–124

Dandekar P., Jain, R., Stauner, T., Loretz, B., Koch, M., Wenz, G., Lehr, C.M. (2012). A Hydrophobic Starch Polymer for Nanoparticle-Mediated Delivery of Docetaxel. *Macromolecular Bioscience, 12,* 184-194.

Ding,Y., Lin,Q., Kan, J. (2018) Development and characteristics nanoscale retrograded starch as an encapsulating agent for colon-specific drug delivery. *Colloids and Surfaces B: Biointerfaces* 171, 656–667.

Griffin, W. C. (1955). Calculation of HLB values of non-ionic surfactants. *Am Perfumer Essent Oil Rev* 65: 26-29.

Haaj, S.B., Magnin, A., Pétrier, C., Boufi, S. (2013). Starch in Food: Structure, Function and Applications. *Carbohydrate Polymers, 92*, 1625.

Jin, H., Zha, C., & Gu, L. (2007). Direct dissolution of cellulose in NaOH/thiourea/urea aqueous solution. *Carbohydrate Research, 342*, 851–858.

Kibar, E.A.A., Gönenç, I., Us, F. (2010) Gelatinization of waxy, normal and high amylose corn starche,

GIDA 35 (4):237-244.

Kim, H.Y., Han J.A., Kweon, D.K., Park, J.D., Lim, S.T. (2013). Effect of ultrasounds treatments on nanoparticles preparation of acid-hydrolized waxy maize starch. Carbohydrate Polymers, 93, 582-588.

Kim, H.Y., Park, D.J., Kim, J.Y. and Lim, S.T. (2013b). Preparation of crystalline starch nanoparticles using cold acid hydrolysis and ultrasonication. *Carbohydrate Polymers, 98(1),* 295–301.

Kim, H.Y., Park, S.S., & Lim, S.T. (2015). Preparation, characterization and utilization of starch nanoparticles. *Colloids and Surfaces B: Biointerfaces, 126*, 607–620.

Kim, J.Y., Park, D.J., Lim, S.T. (2008) Fragmentation of Waxy Rice Starch Granules by Enzymatic Hydrolysis. *Cereal Chemistry, 85(2),* 182–187.

Kumar, S.V., Bafana, A.P., Pawar, P., Rahman, A., Dahoumane, S.A., & Jef, C.S. (2018). High conversion synthesis of < 10 nm starch-stabilized silver nanoparticles using microwave technology. *Scientific Reports, 8*, 5106.

Lamer, V.K., & Dinegar, R.H. (1950). Theory, production and mechanism of formation of monodispersed hydrosols. *Journal of the American Chemical Society, 72*, 11, 4847-4854.

Le Corre, D., Bras, J. & Dufresne, A. (2010). Starch Nanoparticles: A Review. *Biomacromolecules, 11*, 1139–1153.

LeCorre, D., Bras, J., Dufresne, A. (2011). Influence of botanic origin and amylose content on the morphology of starch nanocrystals. *Journal of Nanoparticle Research, 13,* 7193–7208.

Likhitkar, S., Bajpai, A.K. (2012). Magnetically controlled release of cisplatin from superparamagnetic starch nanoparticles. *Carbohydrate Polymers, 87,* 300– 308.

Lin, Q., Ji, N., Li, M., Dai, L., Xu, X., Xiong, L., Sun, Q.(2020) Fabrication of debranched starch nanoparticles via reverse emulsification for improvement of functional properties of corn starch films *Food Hydrocolloids*, 104, 105760.

Lundqvist, H., Eliasson, A.C., & Olofsson, G. (2002a). Binding of hexadecyltrimethylammonium bromide to starch polysaccharides. Part I. Surface tension measurements. *Carbohydrate Polymers*, 49, 43-55.

Lundqvist, H., Eliasson, A.C., & Olofsson, G. (2002b). Binding of hexadecyltrimethylammonium bromide to starch polysaccharides. Part II. Calorimetric study. *Carbohydrate Polymers*, 49, 109-120.

478 Ma, X., Jian, R., Chang, P. R., Yu, J. (2008). Fabrication and characterization of citric acid-modified
479 starch nanoparticles/plasticized-starch composite. *Biomacromolecules, 9(11),* 3314-3320. doi:
480 10.1021/bm800987c.

481 Mathew, A.P. & Dufresne,A. (2002). Morphological investigation of nanocomposites from sorbitol
482 plasticized starch and tunicin whiskers. *Biomacromolecules 3,* 609.

483 Najafi, S.H.M., Baghaie, M., & Ashori, A. (2016). Preparation and characterization of acetylated starch
484 nanoparticles as drug carrier: Ciprofloxacin as a model. *International Journal of Biological*
485 *Macromolecules, 87*, 48–54.

486 Putaux, J.L., Molina-Boisseau, S., Momaur, T and Dufresne, A. (2003). Platelet Nanocrystals Resulting
487 from the Disruption of Waxy Maize Starch Granules by Acid Hydrolysis. *Biomacromolecules, 4,* 1198-
488 1202.

489 Qiu, C., Wang, C., Gong, C., McClements, D.J., Jin, Z. & Wang, J. (2020). Advances in research on
490 preparation, characterization, interaction with proteins, digestion and delivery systems of starch-based
491 nanoparticles. *International Journal of Biological Macromolecules 152,* 117–125.

492 Qiu, Ch., Qin, Y., Zhang, S., Xiong, L., Sun, A. (2016). A comparative study of size-controlled worm-
493 like amylopectin nanoparticles and spherical amylose nanoparticles: Their characteristics and the
494 adsorption properties of polyphenols. *Food Chemistry* 213, 579–587
495 Saari, H., Fuentes, C., Sjöö, M., Rayner, M., & Wahlgren, M. (2017). Production of starch nanoparticles
496 by dissolution and non-solvent precipitation for use in food-grade Pickering emulsions. *Carbohydrate*
497 *Polymers, 157*, 558-566.

498 Schmidts, T., Dobler, D., Guldan, A.C., Paulus, N. & Runkel, F. (2010). Multiple W/O/W emulsions–
499 Using the required HLB for emulsifier evaluation, *Colloid Surf. A-Physicochem Eng. Asp. 372*, 48-54

500 Song, D., Thio, Y.S., Deng, Y. (2011). Starch Nanoparticle formation via reactive extrusion and related
501 mechanism study. *Carbohydrate Polymers, 85,* 211-214.

502 Syahida, I.N., & Subash, G.C.B. (2016). Enhanced antibacterial effect by antibiotic loaded starch
503 nanoparticle. *Journal of the Association of Arab Universities for Basic and Applied Sciences, 24,* 136-
504 140.

505 Tan, Y., Xu, K., Li, L., Liu, C., Song, C. (2009). Wang, Fabrication of size-controlled starch-based
506 nanospheres by nanoprecipitation. *ACS Appl. Mater. Interfaces, (4):956-9.* doi: 10.1021/am900054f.

507 Xiao, S., Tong, Ch., Liu, X., Yu, D., Liu, Q., Xue, Ch., Tang D., & Zhao, L. (2006). Preparation of folate-

conjugated starch nanoparticles and its application to tumor-targeted drug delivery vector. *Chinese Science Bulletin, 51(14),* 1693–1697.